

## Experimental study of transport in a trap-dominated relaxation semiconductor

N. Derhacopian

*Department of Physics, University of California at Los Angeles, Los Angeles, California 90024*

N. M. Haegel

*Department of Materials Science and Engineering, University of California at Los Angeles, Los Angeles, California 90024*

(Received 26 July 1991)

The term "relaxation semiconductor" has been used to define a category of high-resistivity semiconductors in which the dielectric relaxation time exceeds the recombination lifetime ( $\tau_D \gg \tau_0$ ). The transport behavior of semi-insulating GaAs, a trap-dominated relaxation semiconductor, in response to minority-carrier injection has been experimentally investigated. Using a  $p^+ - n - n^+$  structure, the  $I$ - $V$  characteristics have been probed over seven orders of magnitude in current and various regimes have been identified. The experimental results have been compared with previous numerical modeling. A sublinear regime at high bias has been shown to be associated with enhanced trapping by the midgap defects. Impact-ionization processes involving the traps have been demonstrated to be the cause of a sudden rise of current at threshold fields of approximately 1400 V/cm, and the data have been compared to a simple impact-ionization model.

### I. INTRODUCTION AND BACKGROUND

Understanding transport behavior of trap-dominated semiconductors is important both fundamentally and technologically. From a fundamental perspective, traps add several degrees of freedom to the dynamics of charge transport and make possible the observation of various interesting phenomena such as dynamical nonlinearities, instabilities, and chaotic phenomenon,<sup>1</sup> as well as space-charge-limited transport.<sup>2</sup> From a technological point of view, traps in semi-insulating substrates which are used in GaAs microelectronic circuitry lead to a variety of parasitic effects such as side gating, back gating, and unusually long transients.<sup>3</sup>

Both theoretical and experimental investigation of trap-dominated semiconductors offer various complications. Theoretical investigation of transport equations in the trap-dominated semiconductors under minority carrier injection requires the solution of current continuity equations for electrons and holes and Poisson's equation:

$$J_n = qn\mu_n E + qD_n \frac{dn}{dx}, \quad (1)$$

$$J_p = qp\mu_p E - qD_p \frac{dp}{dx}, \quad (2)$$

$$\frac{dE}{dx} = \frac{q}{\epsilon}(p - n + N_t^+), \quad (3)$$

$$\frac{1}{q} \frac{dJ_n}{dx} + G_n - R_n = 0, \quad (4)$$

$$-\frac{1}{q} \frac{dJ_p}{dx} + G_p - R_p = 0, \quad (5)$$

where  $E$  is the electric field,  $J_n$  and  $J_p$  are electron and hole current densities,  $N_t$  is the trap concentration,  $n$  and  $p$  are electron and hole concentrations,  $\mu_n$  and  $\mu_p$  are

electron and hole mobilities,  $D_n$  and  $D_p$  are electron and hole diffusivities, and  $G$  and  $R$  represent generation and recombination terms that may involve midgap defects. An analytical solution of these coupled equations is not possible without some simplifying assumptions. Lampert and Mark, for example, performed an extensive study of injection into high-resistivity semiconductors in which they solved the transport equations by using a "regional-approximation method" where, depending on the region of interest, either the drift or the diffusion component of the current was ignored and an approximate analytical solution was obtained.<sup>2</sup> A more complete description of the problem usually involves computer modeling where the transport equations are solved comprehensively without the omission of any component of current.<sup>4-7</sup>

Experimental investigation of minority-carrier injection into trap-dominated semiconductors is often hampered by poor contact behavior and leakage current problems which naturally arise from the high-resistivity character of the bulk. It is not uncommon to make erroneous conclusions regarding the resistivity of the sample because large near-contact voltage drops dominate the measurement.<sup>8</sup>

One approach to the study of high-resistivity semiconductors was suggested by van Roosbroeck and Casey, who showed that the behavior of a semiconductor under nonequilibrium conditions (i.e., minority-carrier injection) depends on the ratio of two characteristic times: the dielectric relaxation time  $\tau_D$  ( $\tau_D = \rho\epsilon\epsilon_0$ , where  $\rho$  is the resistivity and  $\epsilon$  is the dielectric constant) and the carrier lifetime  $\tau_0$ .<sup>9</sup> They demonstrated that the solution of the equations governing minority-carrier injection into semiconductors produced two distinct solutions depending on whether  $\tau_D/\tau_0 \ll 1$  or  $\tau_D/\tau_0 \gg 1$ . The former was termed the "lifetime regime" and the latter was termed the "relaxation regime."

An alternate way of classifying these two regimes of

transport is by comparing the two characteristic lengths, the Debye length  $L_D$  and the diffusion length  $L_0$ .<sup>10,11</sup> The lifetime regime is defined for the material by the relationship  $L_D \ll L_0$  and the relaxation regime by  $L_D \gg L_0$ . The family of semiconductors that exhibit relaxation-regime behavior potentially include doped or high-purity semiconductors at low temperatures at which the carriers are frozen out, amorphous semiconductors in which high resistivity is due to low mobility, large-band-gap semiconductors in which low carrier concentrations result in high resistivities, and semiconductors with a large concentration of midgap defects that pin the Fermi level in the middle of the band gap, resulting in semi-insulating behavior.

In order to illustrate the difference between the behavior of a *trap-free semiconductor* in the relaxation regime and in the lifetime regime in response to injection of minority carriers, a rather useful graphical method has been devised to elucidate the physics of the problem.<sup>9,12</sup> The hyperbola in Fig. 1 represents a bulk semiconductor in thermal equilibrium (i.e.,  $np = n_i^2$ ). If an  $n$ -type semiconductor, which at equilibrium is represented as point  $A$  on the hyperbola, is perturbed by injection of minority carriers ( $\Delta p > 0$ ), one moves away from the equilibrium hyperbola to some point  $B$ . There are two possible paths back to equilibrium. Path 1 describes the lifetime regime: dielectric relaxation occurs quickly and space charge is neutralized by local enhancement of majority carriers ( $\Delta n > 0$ ) that screen the injected excess minority carriers. As time proceeds, recombination occurs and the system moves back to equilibrium point  $A$ . Path 2 characterizes the relaxation regime: recombination occurs first and

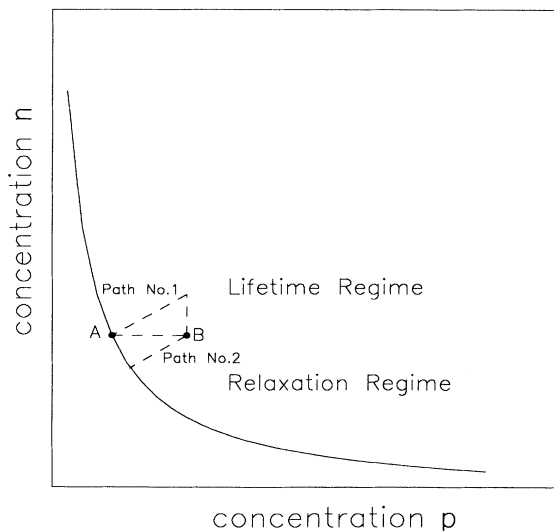


FIG. 1. Schematic diagram showing the "relaxation hyperbola." Point  $A$  on the hyperbola represents an  $n$ -type semiconductor at equilibrium. Immediately after injection of minority carriers (holes), the semiconductor can be represented by point  $B$ . Relaxation to equilibrium occurs via one of two possible paths which characterize the "lifetime regime" or the "relaxation regime."

there is local majority-carrier depletion ( $\Delta n < 0$ ). As time proceeds, dielectric relaxation occurs and excess majority carriers from the bulk neutralize the space charge. This example shows one of the most striking differences between the two regimes: injection of minority carriers into a trap-free semiconductor leads to majority-carrier depletion in the relaxation regime while it leads to majority-carrier augmentation in the lifetime region.<sup>14,15</sup>

This majority-carrier depletion was initially predicted to cause local resistivity increase near contacts upon minority carrier injection.<sup>9</sup> Later analysis of the transport equations, however, revealed that the exclusion of the diffusion component of the current led to this erroneous conclusion.<sup>12,13</sup> An experiment demonstrating majority-carrier depletion associated with minority-carrier injection has been performed on high-purity Si diodes, in which majority-carrier depletion is indicated by the enhancement of diffusion currents. The results of this experiment are in good agreement with the numerical simulation.<sup>14,15</sup>

Henisch and co-workers extended the study of the relaxation regime to include trap-dominated semiconductors.<sup>7,8,16</sup> They used computer modeling and small-signal analysis of the transport equations to show that depletion of majority carriers upon injection of minority carriers is greatly reduced when a large concentration of traps exists. One way of understanding this is to note that in the presence of traps the Debye length  $L_D$  reduces to the screening length  $L_S$ :

$$L_S = \frac{L_D}{\sqrt{1 + N_t/n_0}}, \quad (6)$$

where  $N_t$  is the trap concentration and  $n_0$  is the equilibrium electron concentration. If there is a substantial concentration of midgap defects  $N_t$ , a high-resistivity "relaxation semiconductor" may exhibit lifetime-regime behavior because  $L_S \ll L_0$ . Midgap centers complicate the situation in two general ways. First, they modify the space charge and the electrical-field distribution. Second, they provide an alternate generation-recombination mechanism which affects the lifetime  $\tau_0$ .

Semi-insulating GaAs is an example of a trap-dominated relaxation semiconductor. The characteristic times in this material are  $\tau_D \approx 10^{-5}$  sec (based on  $\rho \approx 10^7 \Omega \text{ cm}$ ) and  $\tau_0 \approx 10^{-10}$  sec at room temperature.<sup>17</sup> This material has a large concentration of mid gap defects known as EL2 ( $N_t \approx 10^{16} \text{ cm}^{-3}$ ), which is generally related to an antisite defect.<sup>18</sup> EL2 is located at 0.67 eV below the conduction band and acts as a donor and an electron trap ( $\sigma_n \approx 4 \times 10^{-16} \text{ cm}^2$ ;  $\sigma_p \approx 2 \times 10^{-18} \text{ cm}^2$ ).<sup>19</sup> It also compensates the shallow acceptors, thereby pinning the Fermi level near the center of the band gap. In typical semi-insulating GaAs  $L_S \approx 10^{-6}$  cm and  $L_0 \approx 10^{-4}$  cm. Therefore it can be seen that even though the material itself has very high resistivity ( $\rho \approx 10^7 \Omega \text{ cm}$  and therefore  $\tau_D \gg \tau_0$ ), one would predict "lifetimelike" behavior (i.e., majority-carrier augmentation in response to injection) since  $L_S \ll L_0$ .

Early experiments on trap-dominated relaxation semiconductors were performed on high-resistivity GaAs

$p$ - $v$ - $n$  structures.<sup>20,21</sup> Extended linear regions in the current-voltage characteristic were observed followed by a sublinear region at high bias which was attributed to depletion of majority carriers upon injection into a relaxation semiconductor.<sup>21</sup> However, as stated previously, subsequent computer modeling showed that the relaxation-regime behavior in the presence of a large concentration of traps does not lead to majority-carrier depletion.<sup>16</sup> Furthermore, theoretical studies of current-voltage characteristics did not show any sublinear region, though it continues to be frequently observed experimentally.<sup>22</sup> The purpose of the present work is to experimentally reassess the problem of injection and transport in trap-dominated relaxation semiconductors.

## II. EXPERIMENTAL METHOD AND RESULTS

The samples used in this work were semi-insulating GaAs  $p^+$ - $v$ - $n^+$  structures. A typical device structure is shown in Fig. 2. Since the material has extremely high resistivity, extra care was taken in preparation of the contacts to the bulk. The injecting  $p^+$  contact was formed by Mg implantation ( $1 \times 10^{14} \text{ cm}^{-2}$  at 60 keV) and the  $n^+$  contact was formed by Si implantation ( $1 \times 10^{14} \text{ cm}^{-2}$  at 60 keV). The implants were then wafer annealed at 900°C for 3 sec. Evaporation of Au-Be on to the  $p^+$  region provided an Ohmic contact while Au-Ge-Ni-Ag was the metallization used on the  $n^+$  region. The contacts were alloyed at 420°C for 30 sec. Wires were connected to the metallic contacts using conducting epoxy. The entire device length was 500  $\mu\text{m}$  and the circular  $p^+$  injecting regions had radii of 500  $\mu\text{m}$ .

To measure the  $I$ - $V$  characteristics, the samples were placed inside an electrically grounded and dark variable temperature cryostat (pressure approximately equal to  $10^{-5}$  Torr). Two different methods were utilized: (1) constant current bias while monitoring the voltage drop across the sample (using a Keithley 220 current source and a Keithley 617 electrometer); (2) constant voltage bias while monitoring the current through the sample (using a Keithley 487 picoammeter and voltage source). The second method reduces the effect of leakage currents which may exist. Both methods yielded similar  $I$ - $V$  characteristics thereby demonstrating the reliability of the structure.

Typical  $I$ - $V$  characteristics of a semi-insulating GaAs  $p^+$ - $v$ - $n^+$  at room temperature are shown in Fig. 3. An extended linear region in the  $I$ - $V$  characteristics is evident over three orders of magnitude up to 8 V (160 V/cm).

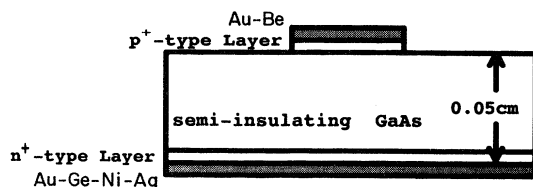


FIG. 2. Schematic representing the  $p^+$ - $v$ - $n^+$  semi-insulating GaAs structure used in the experiment.

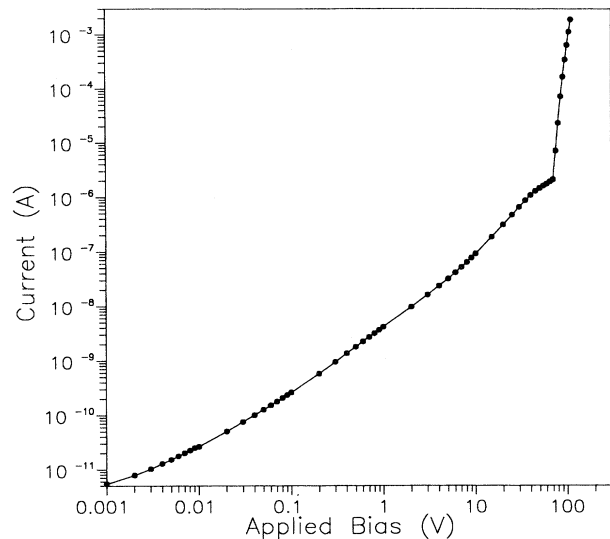


FIG. 3. Current-voltage characteristics of the semi-insulating GaAs  $p^+$ - $v$ - $n^+$  sample used in the experiments.

Then superlinear  $I$ - $V$  characteristics appear, followed by an increase in effective resistance  $R_{\text{eff}}$  [where  $R_{\text{eff}} = (dI/dV)^{-1}$ ]. At an applied bias of approximately 70 V (1400 V/cm) the device switches to a more conducting state and the current increases several orders of magnitude with a small change of applied bias. In fact, we will show that the  $I$ - $V$  characteristics would have indeed gone sublinear had this conducting state not appeared.

In Fig. 4, an extended part of the  $I$ - $V$  characteristics

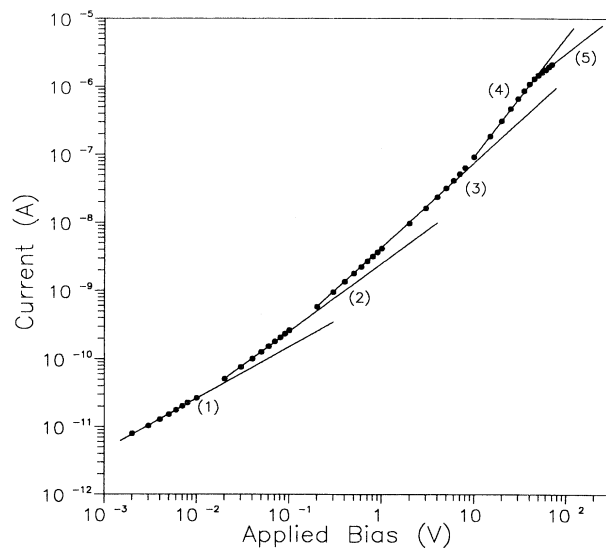


FIG. 4. Experimental current-voltage characteristics of the semi-insulating GaAs  $p^+$ - $v$ - $n^+$  sample (dots) and the curve fits (lines). The first three regions have quasilinear characteristics (region 1,  $I \propto V^{0.8}$ ; region 2,  $I \propto V^{1.0}$ ; region 3,  $I \propto V^{1.2}$ ). Region 4 shows superlinear behavior ( $I \propto V^{1.8}$ ) and it is followed by an increase in  $R_{\text{eff}}$  in region 5.

has been curve fitted by dividing it into five regions. The first three regions have extended quasilinear characteristics which can be fitted by the following equations:

$$\text{region 1, } I = (8.6 \times 10^{-10}) V^{0.8}; \quad (7)$$

$$\text{region 2, } I = (2.5 \times 10^{-9}) V^{1.0}; \quad (8)$$

$$\text{region 3, } I = (4.3 \times 10^{-9}) V^{1.2}. \quad (9)$$

The initial quasilinear regions are followed by a super-linear region which can be approximated by

$$I = (1.6 \times 10^{-9}) V^{1.8}. \quad (10)$$

Finally, a region characterized by an increase in  $R_{\text{eff}}$  can clearly be identified beginning at an applied field of approximately 1000 V/cm and it can be fitted by the equation

$$I = (2.2 \times 10^{-8}) V^{1.1}. \quad (11)$$

The extended quasilinear region has been reported by several authors previously.<sup>21-24</sup> It is characteristic of injection into any high-resistivity semiconductor. At low bias, the effective resistivity has been calculated to be

$$\rho_{I-V, \text{low bias}} = (5.2 \pm 0.3) \times 10^8 \Omega \text{ cm}.$$

Four-point probe measurement on the same sample indicates a bulk resistivity of

$$\rho_{4\text{point}} = (1.1 \pm 0.2) \times 10^8 \Omega \text{ cm}.$$

There is evidence of effective resistivity increase upon injection into this trap dominated relaxation semiconductor. A qualitative explanation for this can be seen in the schematics of Fig. 5 where minority- and majority-carrier profiles have been shown and direction of diffusion and drift components of current for both species have been marked. Figure 5(a) shows the case for a trap-free relaxation semiconductor where depletion of majority carriers causes enhancement of effective conductivity (the diffusion and drift currents of majority carriers are in the same direction). Figure 5(b) shows the extreme case for a trap-dominated relaxation semiconductor where depletion of majority carriers disappears (since  $L_S \ll L_0$ ); the diffusion and the drift components of the majority carriers oppose each other and effective resistivity would increase. It should be noted that this increase of resistivity is due to a local electric-field overshoot near the contact that depends on material parameters such as mobility ratio of minority and majority carriers, sample length, trap cross sections, etc., and its experimental observation may or may not be possible depending on the value of these parameters.<sup>8,22</sup> It is also important to note that resistivity enhancement due to injection should be observed experimentally only at low-bias regime where diffusion plays a more important role.

The  $I-V$  characteristic becomes superlinear at higher bias (10–50 V,  $\beta \approx 1.8$ ). This is expected at high bias where drift dominates over diffusion. Similar behavior has been predicted both analytically and by computer modeling where eventually the material would follow a trap-free square law (where  $\beta = 2.0$ ), which is typical of

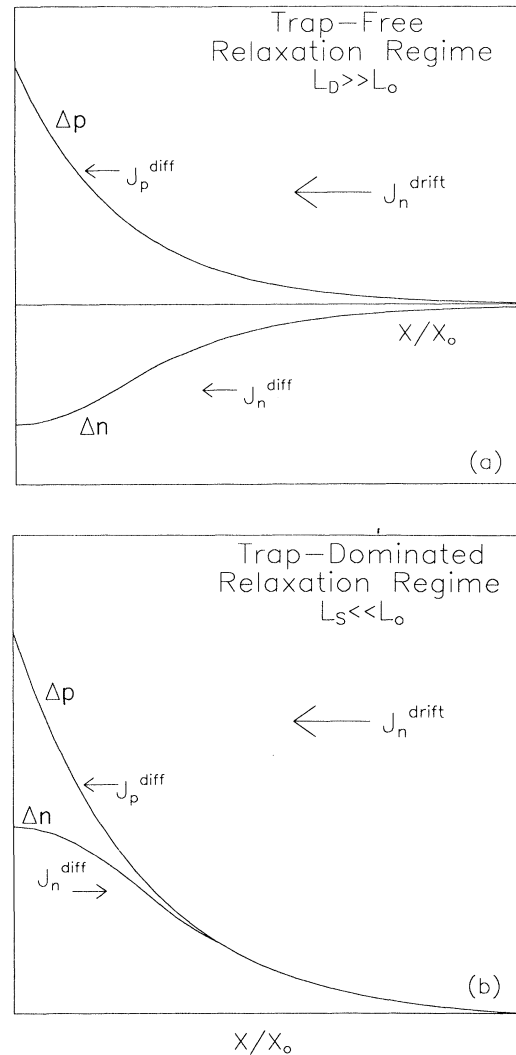


FIG. 5. Schematic diagram showing spatial profiles of minority (holes) and majority (electrons) carriers upon injection of minority carriers into (a) “trap-free relaxation” semiconductor and (b) “trap-dominated relaxation” semiconductor. Directions of the drift and the diffusion components of the current densities are marked. Local conductivity is enhanced in the trap-free case, whereas it is diminished in the trap-dominated case.

high-resistivity semiconductors and insulators.<sup>2,22</sup>

At applied fields in excess of approximately 800 V/cm, the  $I-V$  characteristics tend toward a sublinear region again. This is the result of field-enhanced trapping of electrons by the midgap defect EL2. Hot electrons, with energy  $E \geq 70$  meV relative to conduction-band edge  $E_{\Gamma}$ , are captured more efficiently via a multiphonon process than are electrons in the conduction-band minimum.<sup>25,26</sup> Both differential mobility and effective lifetime will decrease (since the carrier concentration decreases) because of this process and its effect can be seen in the  $I-V$  characteristics as a sublinear region. This effect has been reported by several authors; in certain cases, it is even possible to observe negative differential resistivity (NDR)

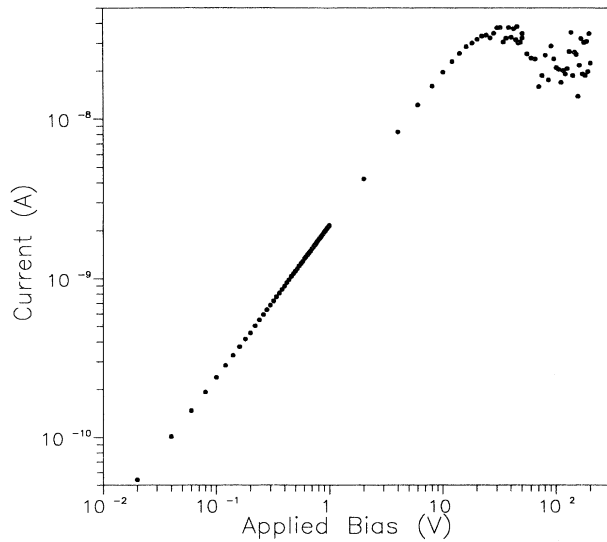


FIG. 6. Current-voltage characteristics in reverse bias. An extended linear region is evident. Above applied fields of approximately 600 V/cm low-frequency oscillations begin.

and low-frequency oscillations (LFO's) that are due to motion of space-charge domains between two electrodes.<sup>25,27,28</sup> In our experiments, we see NDR in reverse bias where the device does not switch to a conducting state (this switching is explained below) and LFO's have been found. Figure 6 shows the reverse-bias  $I$ - $V$  characteristics where at threshold fields of approximately 600 V/cm the  $I$ - $V$  characteristics show the onset of NDR region with LFO's which manifest themselves as apparent scatter in a dc measurement. The low-frequency oscillations are shown in Fig. 7. At a bias of 300 V/cm (open squares) there are no oscillations; at an applied field of 800 V/cm LFO's (dark circles) are clearly present. A more detailed study of these oscillations which are strongly temperature dependent is in progress.

To determine the mobility-lifetime product as a function of applied dc bias, we measured the reverse photocurrent of the  $p^+$ - $v$ - $n^+$  under illumination with above band-gap light (He-Ne laser  $E_{\text{photon}} = 1.96$  eV; power, 1 mW). A segment of the metallization on the circular  $p^+$  layer was etched off to allow light to penetrate the device. The optical absorption coefficient at this wavelength for GaAs is  $\alpha \approx 3 \times 10^4 \text{ cm}^{-1}$  and therefore most of the absorption (electron-hole pair generation) occurs within the first few micrometers.<sup>29</sup> Since the device is reversed biased, the electrons are swept through the bulk to the  $n^+$  electrode under the applied dc field. The holes, however, will remain at the  $p^+$  end and will not traverse the bulk. The role of electrons and holes will be reversed of course if the sample is illuminated from the  $n^+$  side. The photon signal is modulated using a chopper and the modulated photocurrent is detected using a lock-in amplifier. The experimental setup is shown in Fig. 8. The photocurrent can be shown to be given by

$$I_{\text{photo}} = c\mu\tau E_{\text{dc}}, \quad (12)$$

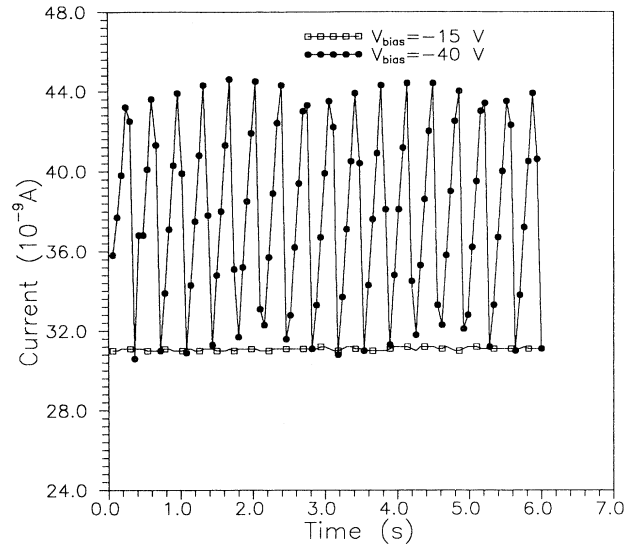


FIG. 7. Reverse bias current as a function of time. At an applied bias of 300 V/cm no oscillations are evident. Low-frequency oscillations can clearly be identified at 800 V/cm.

where  $c$  is a proportionality constant that depends on intensity, quantum efficiency, reflectivity, and absorption coefficient;  $\tau$  is the carrier lifetime;  $\mu$  is the electron mobility; and  $E_{\text{dc}}$  is the applied bias.

Figure 9 shows the normalized  $\mu\tau$  as a function of applied bias. It can be seen that at an applied bias of 800 V/cm the mobility-lifetime product has decreased approximately 17%. This decline, which is due to enhance trapping of electrons by EL2, is believed to be responsible for the sublinear  $I$ - $V$  characteristics. Because the computer modeling of trap-dominated relaxation semiconductors has always considered mobility and lifetime as a constant, it is clear why it has never predicted sublinear behavior observed in the experimental results.<sup>12,18,21,22</sup>

Although other mechanisms, such as the Gunn effect and joule heating, can lead to a decrease of  $\mu\tau$ , these effects may be ruled out as the cause of mobility-lifetime decrease in our case. The Gunn effect has a threshold of 3500 V/cm (175 V for our device) for GaAs and results in extremely high-frequency oscillations, usually in the GHz range. Joule heating in our experiment is negligible due to low currents and low power dissipations. At the onset

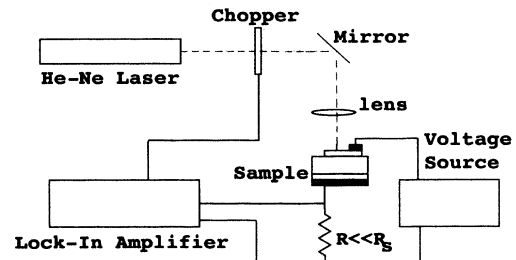


FIG. 8. Experimental setup for the measurement of the mobility-lifetime product.

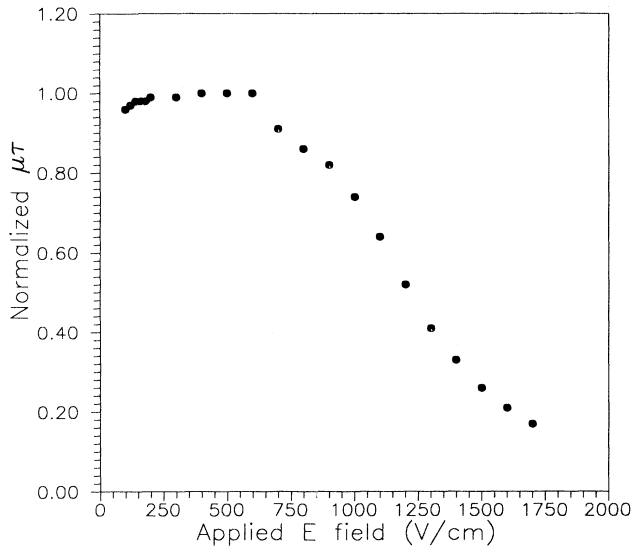


FIG. 9.  $\mu\tau$  as a function of applied bias. At an applied bias of 800 V/cm the mobility-lifetime product has decreased by 17%.

of NDR, for example, power dissipation in the semi-insulating sample was approximately  $10^{-6}$  W. Using a doped GaAs  $p$ - $n$  diode, neither a sublinear region nor NDR behavior was observed in the  $I$ - $V$  characteristics up to  $10^{-3}$  W.

The third significant region of the  $I$ - $V$  characteristics occurs at forward bias at a threshold field of approximately 1400 V/cm and resembles some type of a breakdown mechanism. It should be noted that the steep  $I$ - $V$  characteristic is recoverable and repeatable and does not lead to device degradation. This "breakdown" does not occur in reverse bias and therefore it must depend on the number of carriers in the device. In Fig. 10 this steep section of the  $I$ - $V$  characteristics has been curve fitted using a simple model proposed by Shockley for an impact ionization process.<sup>30</sup> In this model the impact-ionization coefficient  $\alpha$  is related to the applied electric field  $E$  by

$$\alpha = A_1 E \exp\left(\frac{-A_2}{E}\right),$$

where the two fitting parameters  $A_1$  and  $A_2$  are given by  $8.7 \times 10^{-2} \text{ V}^{-1}$  and  $2.5 \times 10^4 \text{ V/cm}$ , respectively. We believe that this effect in the  $I$ - $V$  characteristic is due to impact ionization involving the deep levels since the threshold at which it occurs (1400 V/cm) is much lower than several other possible explanations, such as the trap-filled limit, band-to-band ionization, and Poole-Frenkel effect.<sup>2,29,31-33</sup> Similar conclusions have been reached in other experiments involving semi-insulating GaAs.<sup>32</sup>

### III. CONCLUSION

The  $I$ - $V$  characteristics of a semi-insulating GaAs  $p^+$ - $v$ - $n^+$  structure have been experimentally studied over seven orders of magnitude in current and different re-

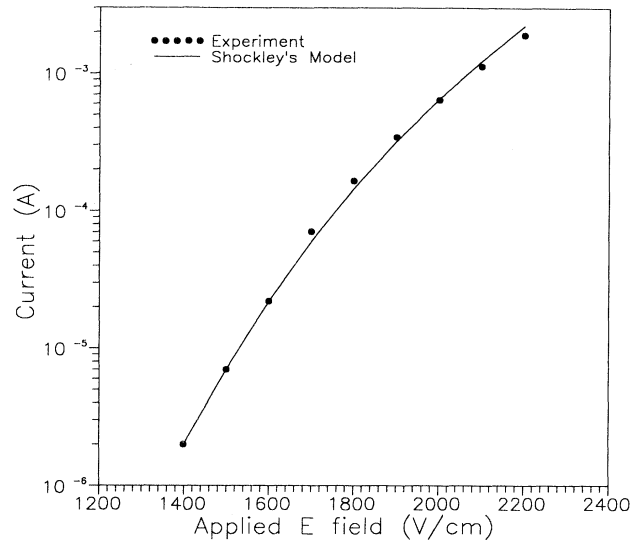


FIG. 10. Current vs applied bias for the steep part of the  $I$ - $V$  characteristics. The experimental data (points) have been curve fitted with an impact-ionization model involving midgap traps.

gions of the  $I$ - $V$  characteristics have been identified. At low applied bias, it is shown that injection of minority carriers into a trap-dominated relaxation semiconductor will not be accompanied by minority-carrier depletion, which is a characteristic of the trap-free case. This result is consistent with earlier numerical modeling and analytical solution of transport equations in the trap-dominated relaxation regime. The sublinear region which appears at high bias is attributed to enhanced trapping by the midgap defects rather than evidence of relaxation-regime behavior as reported earlier.<sup>20</sup> It is also shown that the process, under appropriate conditions, will lead to negative differential conductivity which is accompanied by low-frequency oscillations of the current in the external circuit. At forward bias, impact-ionization processes involving midgap defects are shown to occur at an applied field of 1400 V/cm.

A limited theoretical understanding of injection and transport in space-charge-dominated systems affected earlier interpretation of experimental studies on  $I$ - $V$  characteristics of trap-dominated relaxation semiconductors. The combination of injection, enhanced trapping, and impact ionization, which has been clearly identified here, explains the  $I$ - $V$  characteristics over a wide range of injection levels.

### ACKNOWLEDGMENTS

We would like to thank J. C. Manificier and H. J. Queisser for helpful comments and discussions. We would also like to thank S. Pearton of AT&T Bell Laboratories for the preparation of the samples. One of us (N.D.) would like to acknowledge the expert advice of Z. Sandler of UCLA on subtleties of electronic measurement of high-resistivity materials. This work has been sponsored by NSF Grant No. DMR 8957215 and by the David and Lucile Packard Foundation.

- <sup>1</sup>E. Schöll, *Nonequilibrium Phase Transitions in Semiconductors* (Springer-Verlag, Berlin, 1987).
- <sup>2</sup>M. Lampert and P. Mark, *Current Injection in Solids* (Academic, New York, 1970).
- <sup>3</sup>Y. Ohno and N. Goto, *J. Appl. Phys.* **66**, 1217 (1989). M. Shur, *GaAs Devices and Circuits* (Plenum, New York, 1987), p. 324.
- <sup>4</sup>C. Popescu and H. K. Henisch, *Phys. Rev. B* **11**, 1563 (1975).
- <sup>5</sup>G. H. Döhler and H. Heyszenau, *Phys. Rev. B* **12**, 641 (1975).
- <sup>6</sup>J. C. Manificier and H. K. Henisch, *Phys. Rev. B* **17**, 2640 (1978).
- <sup>7</sup>C. Popescu and H. K. Henisch, *Phys. Rev. B* **14**, 517 (1976).
- <sup>8</sup>H. K. Henisch, *Semiconductor Contacts* (Oxford University Press, New York, 1984).
- <sup>9</sup>W. van Roosbroeck and H. C. Casey, Jr., *Phys. Rev. B* **5**, 2154 (1972).
- <sup>10</sup>J. C. Manificier, Y. Moreau, and R. Ardebili, in *Disorder and Order in Solids*, edited by R. W. Pryor *et al.* (Plenum, New York, 1988), p. 77.
- <sup>11</sup>J. C. Manificier and H. K. Henisch, *J. Phys. Chem. Solids* **41**, 1285 (1980).
- <sup>12</sup>H. K. Henisch, *Philos. Mag. B* **52**, 379 (1985).
- <sup>13</sup>Y. Moreau, J. C. Manificier, and H. K. Henisch, *J. Appl. Phys.* **60**, 2904 (1986).
- <sup>14</sup>B. T. Cavicchi and N. M. Haegel, *Phys. Rev. Lett.* **63**, 195 (1989).
- <sup>15</sup>N. M. Haegel, *Appl. Phys. A* **53**, 1 (1991).
- <sup>16</sup>J. C. Manificier and H. K. Henisch, *J. Appl. Phys.* **52**, 5195 (1981).
- <sup>17</sup>M. Müllenborn, H. Ch. Alt, and A. Heberle, *J. Appl. Phys.* **69**, 4310 (1991).
- <sup>18</sup>G. M. Martin *et al.*, *J. Appl. Phys.* **51**, 2840 (1980).
- <sup>19</sup>J. S. Blakemore, *J. Phys. Chem. Solids* **49**, 627 (1988).
- <sup>20</sup>H. J. Queisser, H. C. Casey, and W. van Roosbroeck, *Phys. Rev. Lett.* **26**, 551 (1971).
- <sup>21</sup>M. Ilegems and H. J. Queisser, *Phys. Rev. B* **12**, 1443 (1975).
- <sup>22</sup>J. C. Manificier and R. Ardebili (unpublished).
- <sup>23</sup>J. Jimenez-Lopez, J. Bonnafé, and J. P. Fillard, *J. Appl. Phys.* **50**, 1150 (1979).
- <sup>24</sup>J. J. Mares, J. Kristofik, V. Smid, and F. Deml, *Solid State Electron.* **31**, 1309 (1988).
- <sup>25</sup>M. Kaminska, J. M. Parsey, J. Lagowski, and H. C. Gatos, *Appl. Phys. Lett.* **41**, 989 (1982).
- <sup>26</sup>B. K. Ridley, and T. B. Watkins, *Proc. Phys. Soc. London* **78**, 293 (1961).
- <sup>27</sup>D. C. Northrop, P. R. Thornton, and K. E. Trezise, *Solid State Electron.* **7**, 17 (1964).
- <sup>28</sup>G. M. Maracas, D. A. Johnson, and H. Goronkin, *Appl. Phys. Lett.* **46**, 305 (1985).
- <sup>29</sup>S. M. Sze, *Physics of Semiconductor Devices* (Wiley-Interscience, New York, 1981), Chap. 1.
- <sup>30</sup>W. Shockley, *Bell. Syst. Tech. J.* **30**, 30 (1951).
- <sup>31</sup>P. T. Landsberg, and D. J. Robbins, *J. Phys. C* **8**, 3825 (1975).
- <sup>32</sup>C. Paracchini and V. Dallacassa, *Solid State Commun.* **69**, 49 (1989).
- <sup>33</sup>M. Jaros, *Deep Levels in Semiconductors* (Hilgar, Bristol, 1982), p. 177.